Molecular Biology of the Cell
Vol. 21, 165–176, January 1, 2010

Molecular Architecture of Synaptic Actin Cytoskeleton in Hippocampal Neurons Reveals a Mechanism of Dendritic Spine Morphogenesis

Farida Korobova and Tatyana Svitkina

Department of Biology, The University of Pennsylvania, Philadelphia, PA 19104

Submitted July 22, 2009; Revised September 28, 2009; Accepted October 23, 2009
Monitoring Editor: Paul Forscher

Excitatory synapses in the brain play key roles in learning and memory. The formation and functions of postsynaptic mushroom-shaped structures, dendritic spines, and possibly of presynaptic terminals, rely on actin cytoskeleton remodeling. However, the cytoskeletal architecture of synapses remains unknown hindering the understanding of synapse morphogenesis. Using platinum replica electron microscopy, we characterized the cytoskeletal organization and molecular composition of dendritic spines, their precursors, dendritic filopodia, and presynaptic boutons. A branched actin filament network containing Arp2/3 complex and capping protein was a dominant feature of spine heads and presynaptic boutons. Surprisingly, the spine necks and bases, as well as dendritic filopodia, also contained a network, rather than a bundle, of branched and linear actin filaments that was immunopositive for Arp2/3 complex, capping protein, and myosin II, but not fascin. Thus, a tight actin filament bundle is not necessary for structural support of elongated filopodia-like protrusions. Dynamically, dendritic filopodia emerged from densities in the dendritic shaft, which by electron microscopy contained branched actin network associated with dendritic microtubules. We propose that dendritic spine morphogenesis begins from an actin patch elongating into a dendritic filopodium, which tip subsequently expands via Arp2/3 complex-dependent nucleation and which length is modulated by myosin II-dependent contractility.

INTRODUCTION

Dendritic spines are small protrusions on the surface of neuronal dendrites that form the postsynaptic component of the excitatory synapse and play important roles in learning and memory. Alterations in dendritic spines are found in many types of mental retardation and other neurological disorders (Calabrese *et al*., 2006). By morphology, dendritic spines are usually classified as mushroom shaped, thin (or elongated), and stubby, and their shape is thought to correlate with the strength and activity of the synapse (Bourne and Harris, 2008). A mushroom spine has a bulbous head connected to the dendrite by a constricted neck (or stalk); thin spines have a smaller head, and stubby spines lack a neck. However, these categories are not separated by clear-cut boundaries but rather describe a continuum of shapes (Arellano *et al*., 2007). A distinctive feature of dendritic spines is the postsynaptic density (PSD), a large assembly of receptors and signaling proteins associated with the membrane of the spine head at the junction with a presynaptic bouton of the axon (Fifkova and Delay, 1982; Sheng and Hoogenraad, 2007).

Dendritic spines are highly dynamic (Matus, 2005) and their formation, maturation, and plasticity heavily depend on the actin cytoskeleton remodeling (Ethell and Pasquale, 2005; Cingolani and Goda, 2008). However, the underlying mechanisms and even the structural organization of actin filaments in spines are poorly understood (Halpain, 2000; Rao and Craig, 2000; Ethell and Pasquale, 2005; Tada and Sheng, 2006), apparently because of their small size combined with complex organization. These features critically require electron microscopy (EM) to fully understand the biology of dendritic spines.

The major types of actin filament organization across cell types and subcellular organelles include protrusive structures, such as branched networks in lamellipodia (Svitkina *et al*., 1997; Svitkina and Borisy, 1999) and parallel bundles in filopodia (Svitkina *et al*., 2003), and contractile structures, such as bundles and networks of linear filaments with mixed polarity (Verkhovsky *et al*., 1995). Early EM studies of dendritic spines by using thin-section (Fifkova and Delay, 1982; Markham and Fifkova, 1986) or freeze-fracture (Landis and Reese, 1983; Hirokawa, 1989) techniques detected long filaments, as well as a meshwork of short, potentially branched, actin filaments in spines, but they failed to provide a cohesive picture of their entire cytoskeleton. More recent light microscopic and functional approaches revealed that proteins normally involved in generation of protrusive branched networks, such as the Arp2/3 complex (Racz and Weinberg, 2008), WAVE1 (Kim *et al*., 2006; Hotulainen *et al*., 2009), cortactin (Hering and Sheng, 2003), N-WASP (Wegner *et al*., 2008), profilin (Ackermann and Matus, 2003), and cofilin (Racz and Weinberg, 2006; Hotulainen *et al*., 2009), were present in spines. However, myosin II (Cheng *et al*., 2000; Ryu *et al*., 2006) and α-actinin (Wyszynski *et al*., 1997) were also found there suggesting formation of contractile bundles or networks. Kinetically, dendritic spines contain dynamic and stable subpopulations of actin (Honkura *et al*., 2008), which may correspond to distinct types of actin fila-

This article was published online ahead of print in *MBC in Press* (http://www.molbiolcell.org/cgi/doi/10.1091/mbc.E09–07–0596) on November 4, 2009.

Address correspondence to: Tatyana M. Svitkina (svitkina@sas.upenn.edu).

Abbreviations used: DIV, days in vitro; EM, electron microscopy; PSD, postsynaptic density.

ment arrays within spines. In general, a common belief is that the head of a spine should be similar to lamellipodia and contain an Arp2/3 complex-dependent branched network, whereas the spine neck is probably maintained by an axial actin filament bundle (Halpain, 2000; Rao and Craig, 2000; Tada and Sheng, 2006; Hotulainen *et al*., 2009). However, these ideas have not been directly proven and the actin filament organization in spines remains uncertain. Even less is known about the structure of presynaptic actin, which is believed to have a dual function of restraining synaptic vesicles and of directing them toward the synapse (Cingolani and Goda, 2008).

Dendritic spines are thought to derive from dendritic filopodia that establish the initial contact with an axon, although other models also exist (Papa *et al*., 1995; Ethell and Pasquale, 2005; Yoshihara *et al*., 2009). The cytoskeletal organization and molecular composition of dendritic filopodia remain totally unknown. They may be similar to conventional filopodia found in neuronal growth cones and at the leading edge of other migrating cells that contain a tight bundle of long uniformly oriented actin filaments in their interior (Small *et al*., 2002; Svitkina *et al*., 2003; Korobova and Svitkina, 2008). Alternatively, dendritic filopodia may be structurally similar to dendritic spines (Papa *et al*., 1995), which structure as mentioned earlier is also unknown. These conflicting considerations require an experimental approach to investigate the actual structure of dendritic filopodia.

Here, we used platinum replica EM to characterize the cytoskeletal organization and molecular composition of dendritic spines and dendritic filopodia in dissociated cultures of hippocampal neurons and revealed novel features of both structures essential for understanding of their morphogenesis and dynamics.

MATERIALS AND METHODS

Cell Culture and Transfection

For high density cultures, hippocampal neurons were isolated as described previously (Wilcox *et al*., 1994) and were kindly provided by Dr. M. Dichter (The University of Pennsylvania, Philadelphia, PA). Every 5 d, one third of culture medium was replaced by fresh medium. For transfection with enhanced yellow fluorescent protein (EYFP)-actin (Clontech, Mountain View, CA) or mCherry-actin (Yang *et al*., 2009), hippocampal neurons were plated on 35-mm glass-bottomed dishes at 100,000 cells/dish concentration and transfected using Lipofectamine 2000 (Invitrogen, Carlsbad, CA) after 5–6 days in vitro (DIV). Transfected cells were analyzed on 14 DIV.

Antibodies

The following rabbit polyclonal antibodies were used: p16-Arc (Vignjevic *et al*., 2003), Arp3 (Santa Cruz Biotechnology, Santa Cruz, CA), and p34-Arc subunits of Arp2/3 complex (Millipore, Billerica, MA), nonmuscle myosin II from bovine spleen (Verkhovsky *et al*., 1987), and capping protein (from D. Schafer, University of Virginia). The following mouse monoclonal antibodies were used: fascin (Millipore), microtubule-associated protein (MAP2) (Sigma-Aldrich, St. Louis, MO), N-cadherin (Santa Cruz Biotechnology; gift from W. J. Nelson, Stanford University, Stanford, CA), α-tubulin (Sigma-Aldrich), and PSD-95 (Abcam, Cambridge, MA). Secondary fluorescently labeled antibodies and AlexaFluor 488-, 594-, and 647-labeled phalloidins were from Invitrogen, secondary rabbit or mouse antibodies conjugated to 12- or 18-nm colloidal gold were from Jackson ImmunoResearch Laboratories (West Grove, PA).

Immunofluorescence and Light Microscopy

Immunofluorescence staining of cells growing on glass coverslips was performed after cell extraction for 5 min with 1% Triton X-100 in PEM buffer [100 mM piperazine-*N*,*N*′-bis(2-ethanesulfonic acid)-KOH, pH 6.9, 1 mM $MgCl_2$, and 1 mM EGTA] containing 2% polyethelene glycol (mol. wt. 35,000) and 5 μM phalloidin and fixation with 4% paraformaldehyde in phosphate-buffered saline (PBS) or 0.2% glutaraldehyde in 0.1 M Na-cacodylate, pH 7.3. Glutaraldehyde-fixed samples were quenched with 2 mg/ml $NaBH_4$. For F-actin staining, fluorescently labeled phalloidin (0.033 μM) was added to the secondary antibody solution. For fascin immunostaining, extracted cells were fixed with 50% methanol in PBS and washed with PBS. For time-lapse imaging, cells were cultured in glass-bottomed dishes and kept on the microscope stage in the TC-MIS-20 × 46 miniature incubator (Bioscience Tools, Santa Clara, CA) at 36.5°C in the atmosphere containing 5% CO_2 and 20% O_2. For correlative immunostaining, marked coverslips were used to help with cell identification (Svitkina, 2007). Immediately after acquisition of 10- to 12-min-long movies with 2- to 3-s time intervals, the medium in the dish was changed to 4% paraformaldehyde in PBS, and cells were immunostained as described above. Light microscopy was performed using an inverted microscope (Eclipse TE2000; Nikon, Tokyo, Japan) equipped with Planapo 100 × 1.3 numerical aperture or 20 × 0.75 objectives and Cascade 512B charge-coupled device (CCD) camera (Roper Scientific, Trenton, NJ) driven by MetaMorph imaging software (Molecular Devices, Sunnyvale, CA).

Electron Microscopy

Samples for platinum replica EM, correlative light and electron microscopy, immuno-EM, and S1 decoration were processed as described previously (Svitkina, 2007; Korobova and Svitkina, 2008). For nonextracted samples, neuronal cultures were fixed sequentially with 2% glutaraldehyde in Na-cacodylate, and with aqueous solutions of 0.2% uranyl acetate, 0.1% tannic acid, and 1% OsO_4. For Arp2/3 complex immunogold staining, cells were extracted as for immunofluorescence, fixed with 0.2% glutaraldehyde, quenched with $NaBH_4$, and incubated in a mixture of p16-Arc, Arp3, and p34-Arc antibodies. For N-cadherin, myosin II, and capping protein immunostaining, unfixed cells extracted with 1% Triton X-100 and 4% polyethelene glycol in PEM buffer were incubated for 15 min with a primary antibody in the PEM buffer containing 5 μM unlabeled phalloidin, washed with the PEM buffer, fixed with 0.2% glutaraldehyde, stained with secondary antibody, and postfixed with 2% glutaraldehyde. For PSD-95 staining, cells were extracted/fixed for 5 min with a mixture of 0.5% Triton X-100 and 1% paraformaldehyde in PEM buffer with 5 μM phalloidin, washed in the same buffer, incubated with primary antibodies in PEM buffer for 15 min, postfixed with 2% glutaraldehyde, and stained with secondary antibody. Myosin S1 (gift from Dr. L. Tilney) was centrifuged at 100,000 × *g* for 30 min before use. For correlative light and electron microscopy, EYFP- or mCherry-actin–expressing cells were located on marked glass-bottomed dishes and phase-contrast and fluorescent images were acquired immediately before extraction and within 2 min after addition of the extraction solution. Then cells were fixed and processed for EM, as described previously (Svitkina, 2007; Korobova and Svitkina, 2008). Samples were analyzed using JEM 1011 transmission EM (JEOL USA, Peabody, MA) operated at 100 kV. Images were captured by ORIUS 835.10W CCD camera (Gatan, Warrendale, PA) and presented in inverted contrast. Identification of gold particles in replica EM samples was performed at high magnification after contrast enhancement to distinguish them from other bright objects in the samples. Thus, gold particles showed up as solid white circles in contrast to filament ends, for example, which usually have a donut-like appearance.

Image Analysis and Statistics

All morphometric measurements were done using MetaMorph or Photoshop (Adobe Systems, Mountain View, CA) software packages and repeated for at least two independent experiments. Data were analyzed using Excel software (Microsoft, Redmond, CA). Significance was determined using a two-tailed *t* test. For quantification of F-actin and Arp2/3 complex contents in filopodia, filopodia were manually selected on phalloidin-stained images using the MetaMorph selection tool and selection was transferred to corresponding Arp2/3 complex-stained images. Average fluorescence intensities of selected regions from both sets of images were recorded after background subtraction.

To quantify the distribution of PSD-95 and N-cadherin immunogold labeling in dendritic spines relative to the adjacent axon, we measured the shortest distances between individual gold particles and the nearest microtubule or intermediate filament in the axonal shaft in EM samples. Gold particles occurring on the other side of the first axonal fiber were assigned negative numbers. Only gold particles located in the distal half of the spine, were included into quantification to exclude irrelevant labeling in the dendritic shafts where both PSD-95 and N-cadherin are also present. If the axon and the dendrite were not parallel, the distal half of the spine was determined by drawing a bisector for the angle between them until it intersects the spine.

RESULTS

Identification of Spines

Platinum replica EM is advantageous for investigation of the cytoskeletal organization of whole-mount samples at high resolution (Svitkina, 2007). However, detergent extraction, which is required for this technique, dissolves membranes making cell boundaries undetectable and has a potential to perturb the cytoskeletal organization. Therefore, we performed control experiments to identify dendritic spines, de-

termine their polarity, and test their preservation in EM samples.

First, we performed replica EM of nonextracted hippocampal neurons in which cell boundaries remain preserved (Figure 1). Neurites in these cultures usually formed complex networks or aligned bundles (Figure 1A). Dendritic spines were abundant in mature cultures fixed after 14–28 DIV and could be recognized by their mushroom shape and/or ability to make contacts (presumably, synapses) with adjacent neurites (Figure 1, A–D). An axon interacting with the spine head was usually thinner than the dendrite, from which the spine emerged. The spine necks frequently expanded not only at the tip forming a bulbous head, but also at the root, although to a lesser extent, forming a delta-shaped base (Figure 1C). At 7–11 DIV, spines were rare, but dendritic filopodia abundant (Figure 1, E–H). Compared with straight and uniform growth cone filopodia in the same samples (data not shown), dendritic filopodia were very polymorphic. Occasionally, they made contacts with other neurites (Figure 1H). At this stage of development, dendrites also formed small lamellipodia-like protrusions (data not shown).

We also stained hippocampal cultures with a dendritic marker MAP2 (Caceres *et al*., 1984) and phalloidin to distinguish dendrites and axons (Supplemental Figure S1). A strong MAP2 signal in dendrites correlated with prominent F-actin staining and a greater thickness of neurites; in contrast, MAP2-depleted axons contained much less F-actin and were on average thinner.

Finally, we used correlative EM of EYFP-actin–expressing neurons to visualize the same spines sequentially by light and EM (Supplemental Figure S2). These results showed that detergent extraction and EM processing did not alter the shape or actin distribution in spines. They also revealed characteristic features of the spine cytoskeleton, such as a greater density of the actin filaments in spine heads, compared with spine bases.

Based on these experiments, we applied following criteria to identify the spine polarity in EM samples (Supplemental Figure S3): a greater thickness of dendrites and abundance of actin filaments there, compared with axons; a greater size and higher actin filaments density in spine heads, as compared with bases; and a more distinct delta-like shape of bases, as compared with more polymorphic heads.

Actin Cytoskeleton Organization in Dendritic Spines

Mature 14–28 DIV hippocampal neurons were used for EM analysis of dendritic spines. Axons and dendrites could be recognized by axial bundles of microtubules and intermediate filaments in their interior, and dendrites also contained significant amount of actin filaments (Supplemental Figure S3). A typical mushroom spine contained three compartments: a bulbous head contacting the axon, a constricted neck in the middle, and a delta-shaped base at the junction with the dendrite (Figures 2 and 3 and Supplemental Figure S3).

The spine head typically contained a dense network of short cross-linked actin filaments, in which branched filaments were clearly visible in relatively sparse regions (Figure 2A). Long filaments were also sometimes observed in the spine head. Surprisingly, the actin network in the dendritic spine head seemed to directly interact with axonal microtubules and intermediate filaments (Figure 2). Proximity of actin-rich spine heads to microtubules in the axon was also seen by fluorescence microscopy (Supplemental Figure S4). However, part of this network likely belongs to the presynaptic bouton, rather than to the dendritic spine (see below). Accordingly, occasional chunks of nonfibrillar material in the spine head, which might represent nonextracted PSD fragments, were found either next to the axonal micro-

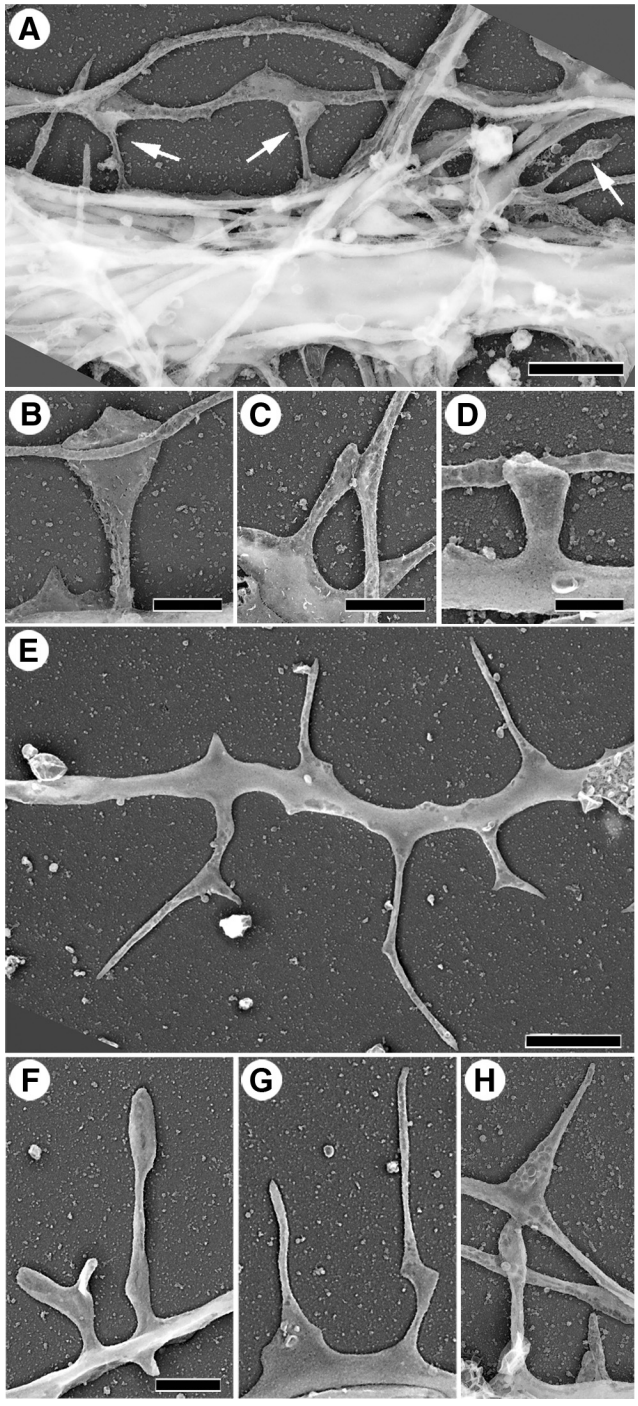

Figure 1. Morphology of dendritic spines (A–D) and dendritic filopodia (E–H). Replica EM of nonextracted hippocampal neurons after 14 (A–D) or 10 (E–H) DIV. (A) Network of neurites with dendritic spines (arrows); two spines contact other neurites (axons). The cell body producing the major dendrite is located ~20 μm away from the left margin of the panel. (B–D) Examples of mushroom (B), thin (C), and stubby (D) spines. (E) Distal region of a dendrite with polymorphic dendritic filopodia. (F–H) Examples of dendritic filopodia. Bars, 2 μm (A and E), 1 μm (B–D, F, and G), or 0.5 μm (H).

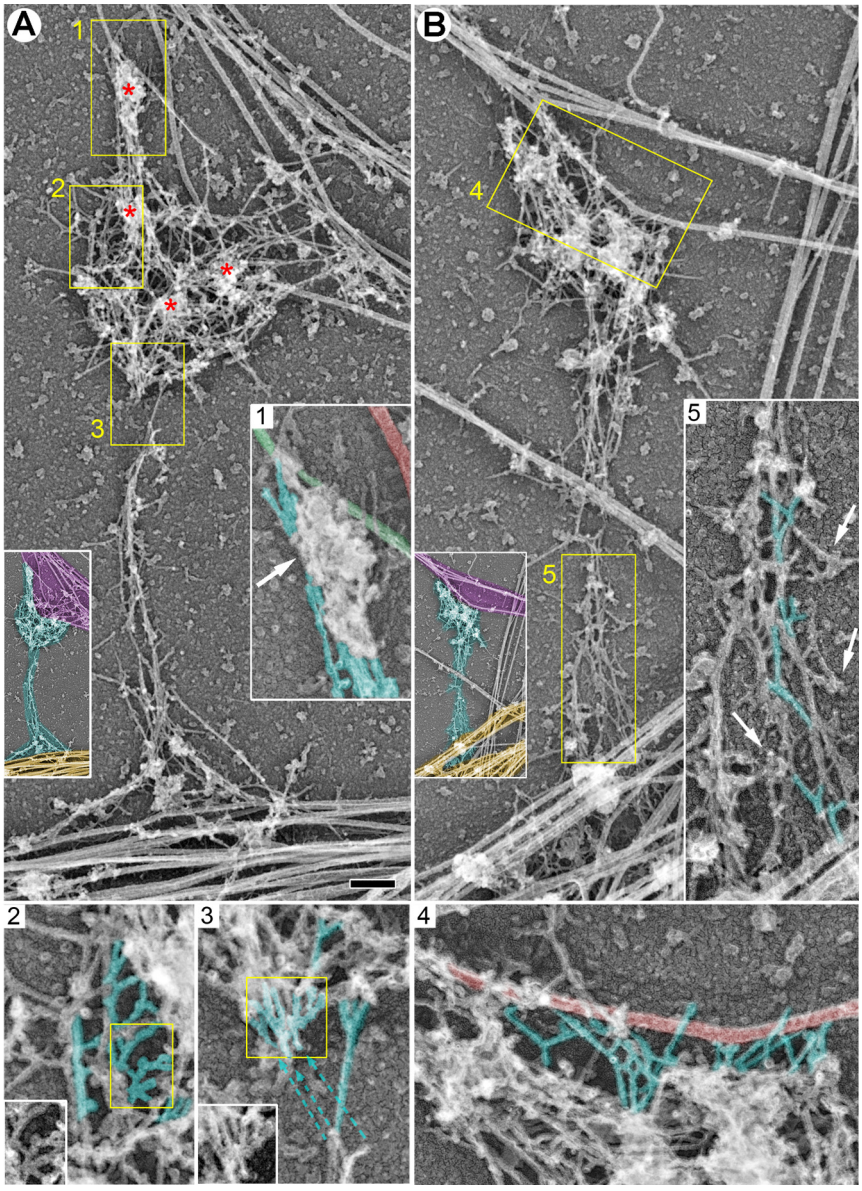

Figure 2. Cytoskeletal organization of dendritic spines: head and neck. EM of extracted 14 DIV neurons. Mushroom (A) and thin (B) spines associate with dendrites at the base (bottom) and with axons by the head (top). Unlabeled insets show the smaller versions of the corresponding main panels with axons color-coded in purple, dendrites in yellow, and spines in cyan. See Supplemental Figure S3 for determination of the orientation of the spine shown in A. Thick fibers in both neurites represent microtubules. Red asterisks indicate putative PSD fragments. Yellow boxes are enlarged in panels with corresponding numbers. Box 1, interaction of putative PSD (arrow) from the spine head with axonal intermediate filaments (green); actin filaments are shown in cyan and a microtubule in red. Boxes 2, 3, and 5, branched actin filaments (cyan) in the head (2), at the neck–head junction (3), and in the neck (5) of respective spines. Insets in panels 2 and 3 show nonpseudocolored regions outlined by yellow boxes. Dashed arrows in panel 3 indicate potential filament breakage. Box 4, interaction of actin filaments (cyan) with an axonal microtubule (red). Bars, 0.2 μm (A and B).

tubules and intermediate filaments, or slightly away from them (Figure 2A).

In the spine neck, actin filaments formed an anisometric network, which consisted of loosely arranged actin filaments that might be longitudinally oriented, but only infrequently formed tight bundles. The number of filaments varied significantly along the length of the neck and many filaments did not span the entire neck. Filaments began or ended with unbound ends but also branched off of the side of another filament (Figure 2B). At the neck–head junction, the number of actin filaments abruptly increased toward the head, which usually occurred through extensive branching of neck filaments entering the head (Figure 2A).

The spine base is a previously unrecognized structural compartment of the spine. It usually contained relatively long actin filaments converging from a broad area in the dendrite toward the neck in a delta-shaped configuration (Figures 2 and 3). These filaments either continued into the neck, or terminated within the base (Figure 3C). In many spines, the base also contained branched filaments (Figure 3A). Surprisingly, the actin filaments of the spine base frequently seemed to begin directly from the microtubule network in the dendrite and subsequently amplified through branching (Figures 2 and 3), whereas others originated from other actin structures in the dendrite. Some spines did not have a well-formed base (Figure 3B).

Other morphological types of spines displayed the same structural plan. However, thin spines (Figure 2B) had longer necks and narrower heads, whereas stubby spines seemed to lack a neck and consisted of a patch of a densely branched actin network that likely represented the spine head or a merge of the base and the head (Figure 3B). The dimensions of spine compartments varied broadly even within one morphological class of spines blurring the distinction between the classes. Some mushroom-shaped dendritic protrusions not making contacts with axons had nonetheless a similar structural organization as the contact-forming spines (data not shown). Decoration of actin filaments with the myosin II subfragment 1 (S1) confirmed that actin filaments were the major cytoskeletal component of spines (Figure 3C). How-

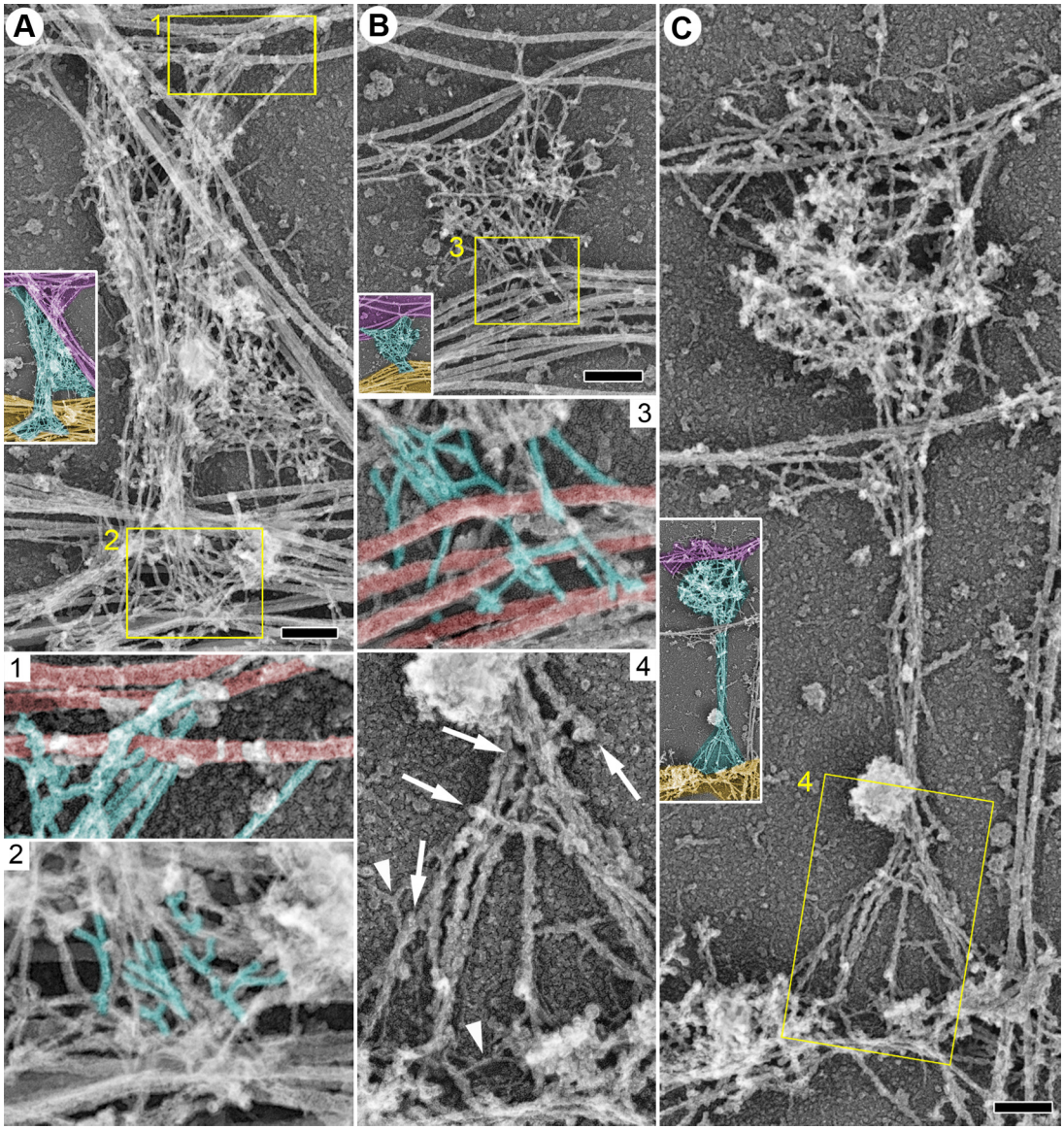

Figure 3. Cytoskeletal organization of dendritic spines: base. EM of extracted neurons after 11 (A) or 14 (B and C) DIV shows undecorated (A and B) or S1-decorated (C) mushroom (A and C) or stubby (B) spines. The spine in A also may be considered stubby. Unlabeled insets show the smaller versions of the corresponding main panels with axons color-coded in purple, dendrites in yellow, and spines in cyan. Yellow boxes are enlarged in panels with corresponding numbers. Box 1, interaction of actin filaments (cyan) with axonal microtubules (red). Boxes 2 and 3, branched actin filaments (cyan) in the spine bases associate with dendritic microtubules (red). Box 4, linear actin filaments in the spine base have unbound ends (arrows) and are arranged in a delta-shaped configuration. S1-decorated actin filaments have a rough bumpy outline that distinguishes them from undecorated thin filaments (arrowheads). Bars, 0.2 μm (A–C).

ever, nondecorated filaments of ~ 6 nm in thickness (including an ~4-nm platinum layer) were also detected in different spine compartments (Figure 3C).

Thus, the cytoskeletons of the head, neck, and base of a mature spine are not dramatically different from each other and consist of a mixture of branched and linear filaments, but in different combinations. Branched filaments dominate in the head, whereas linear filaments are more prominent in the base, and the neck may contain different ratios of both. The mutual alignment of actin filaments also varies between compartments being most prominent in the neck, but not to an extent of forming a tight bundle. This organization is conserved among all spine classes, mushroom, thin and stubby, but the dimensions of individual compartments vary broadly up to complete absence of a neck and/or a base.

Molecular Markers in Dendritic Spines

The presence of branched actin networks in different spine compartments suggested involvement of the Arp2/3 complex. Indeed, immunofluorescence staining detected Arp2/3 complex in the majority of heads and in 30–40% of necks and bases of mushroom or thin spines (Figure 4, A and D). In stubby spines, the Arp2/3 complex was found throughout the spine. Small actin patches that were usually present in dendrites also contained the Arp2/3 complex. Immunolocalization of another common marker of branched networks, heterodimeric capping protein (Svitkina *et al.*, 2003),

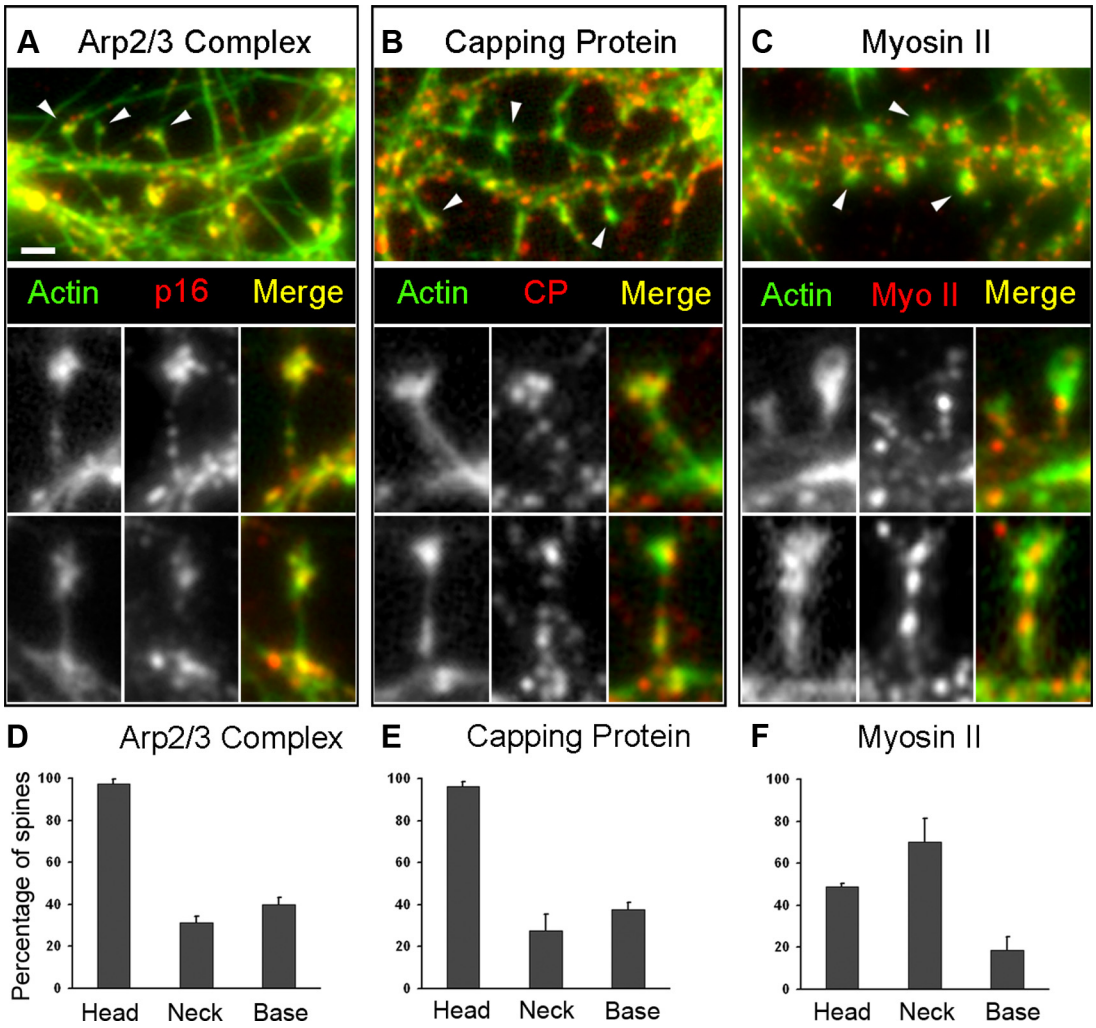

Figure 4. Immunofluorescence staining of cytoskeletal proteins in spines. (A–C) Low-magnification (top) and high-magnification (bottom) images of dendritic spines in 14 DIV hippocampal neurons stained with phalloidin (green) and indicated antibodies (red). Dendritic spines are marked by arrowheads. (D–F) Percentage of spine compartments immunopositive for indicated proteins in the population of spines. Data are collected from three experiments and expressed as mean ± SD (137 spines for the Arp2/3 complex; 90 spines for capping protein, and 121 spines for myosin II). Bars, 2 μm (A–C).

gave similar results (Figure 4E). An actin filament cross-linker, fascin, which is characteristic for conventional filopodia (Svitkina *et al*., 2003), was virtually absent from dendritic spines (Supplemental Figure S5).

Apparently seamless transition between dendritic and axonal cytoskeletons at the synaptic junction in the detergent-extracted samples prompted us to attempt to elucidate the position of a boundary between two cells using immuno-EM of N-cadherin, a transmembrane junctional molecule involved in synapse formation (Bourne and Harris, 2008), and PSD-95, a scaffolding protein in the PSD that has perijunctional localization (Tada and Sheng, 2006). As expected for the membrane-associated molecules, a significant fraction of both proteins was dissolved by the detergent treatment during immuno-EM processing, but a fraction of them remained. Although labeling was not dense, it was specific, as gold particles were not detected in inappropriate locations and they were absent when primary antibodies were omitted. Furthermore, the staining pattern was consistent between spines and experiments. Gold particles in both cases tended to localize at some distance from axonal microtubules and intermediate filaments within the actin network in spine "heads" (Figure 5A and Supplemental S6). Because the intensity of labeling was limited to approximately five to six gold particles per spine, it was not possible to precisely demarcate the interface between the axon and the spine in each individual case. Therefore, to quantitatively evaluate the label distribution and thus an average position of the boundary, we measured the distance between gold particles labeling N-cadherin or PSD-95 and the closest definite cytoskeletal component of an axon, usually a microtubule or an intermediate filament. The quantification produced similar results for both markers. Thus, gold particles labeling N-cadherin and PSD-95 were localized at distances of 264 ± 417 nm (mean ± SD; 10 spines, 59 gold particles) and 287 ± 382 nm (12 spines, 60 gold particles) from axons, respectively, supporting an idea that a fraction of the actin network at the spine tips, in the order of several hundreds nanometers, probably belongs to the axon rather than to the dendrite. The structure of the network was similar on the both sides of the putative boundary revealed by the N-cadherin or PSD-95 labeling. Additional gold particles of N-cadherin staining were also found in dendrites consistent with frequent bundling of dendrites in these cultures (Figure 1A).

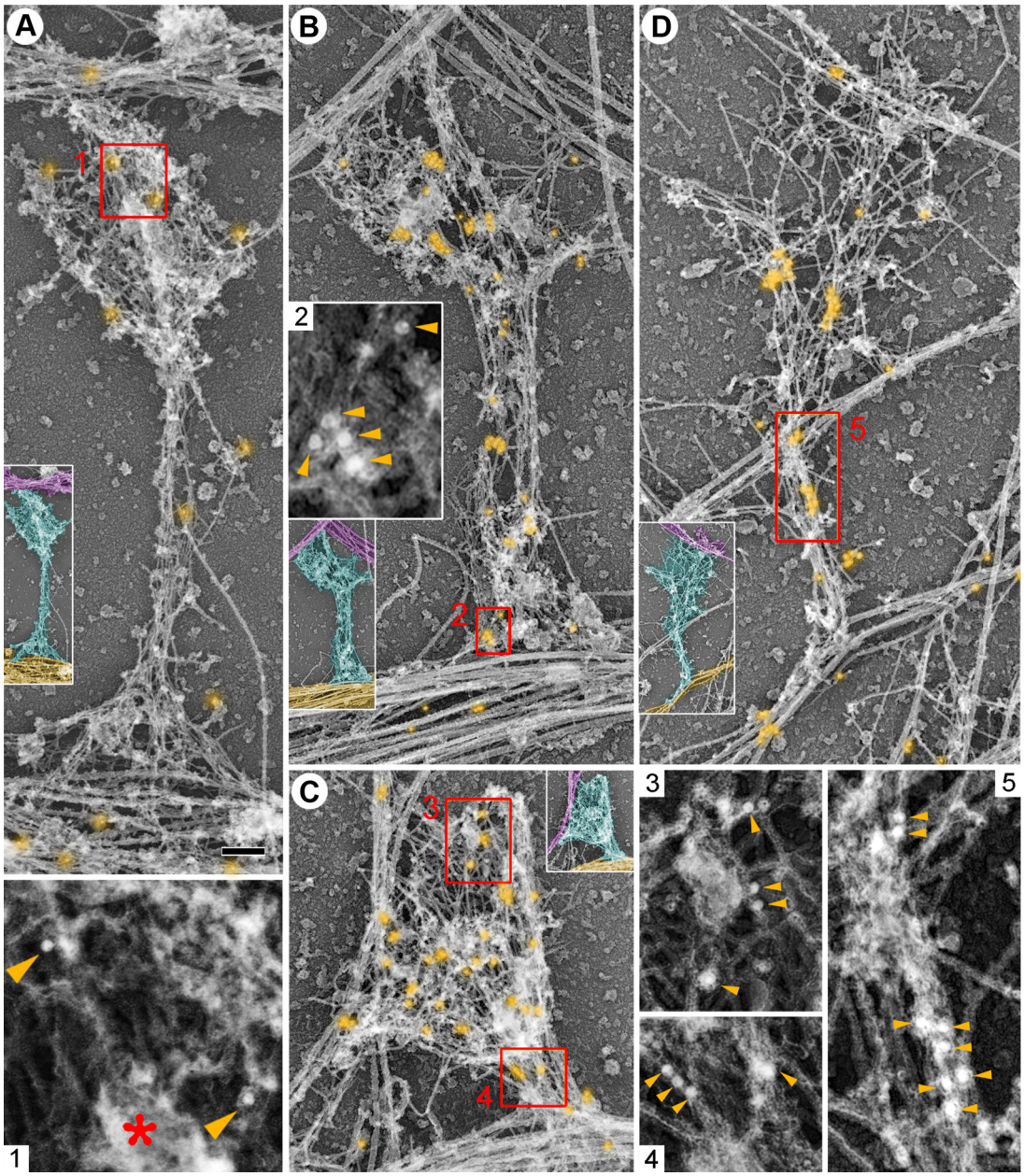

Figure 5. Immunogold EM of cytoskeleton-associated proteins in spines. Unlabeled insets show the smaller versions of the corresponding main panels with axons color-coded in purple, dendrites in yellow, and spines in cyan. (A) N-cadherin. (B) Arp2/3 complex. (C) Capping protein. (D) Myosin II. Gold particles showing protein localization are highlighted in orange. Red boxes are enlarged in panels with corresponding numbers to show noncolorized gold particles (arrowheads). Box 5 shows a linear cluster of gold particles at the bottom. Bar, 0.2 μm.

Immunogold EM of Arp2/3 complex and capping protein gave similar results (Figure 5, B and C) and showed that all analyzed mushroom or thin spines (N = 23 and 22 spines for Arp2/3 complex and capping protein, respectively) contained gold particles in the head, and approximately half of spines was labeled in the neck (11 and 14 spines, respectively) and the base (13 spines for each protein). The density of gold particles in necks and bases was usually lower, than in heads. Stubby spines had even distribution of gold particles throughout the body.

Next, we evaluated the precise distribution of myosin II in spines, which presence in spines was reported previously (Morales and Fifkova, 1989; Ryu *et al*., 2006). Immunofluorescence staining revealed a punctate, or sometimes diffuse, distribution of myosin II in dendritic spines, dendrites, and the cell body (Figure 4, C and F). Myosin puncta likely corresponded to myosin II bipolar filaments (Verkhovsky *et al*., 1995), whereas diffuse staining might correspond to individual cytoskeleton-associated myosin II molecules. In spines, myosin II puncta predominantly localized to the neck and a lower part of the head, and to a lesser extent to the base.

Immunogold EM revealed similar distribution of myosin II between spine compartments (Figure 5D). Thus, of 11 mushroom or thin spines analyzed, the neck (10 spines) and the lower part of the head (9 spines) were most frequently labeled, whereas the base labeling was less frequent (5 spines). However, gold particles in the neck frequently formed linear clusters, possibly reflecting formation of my-

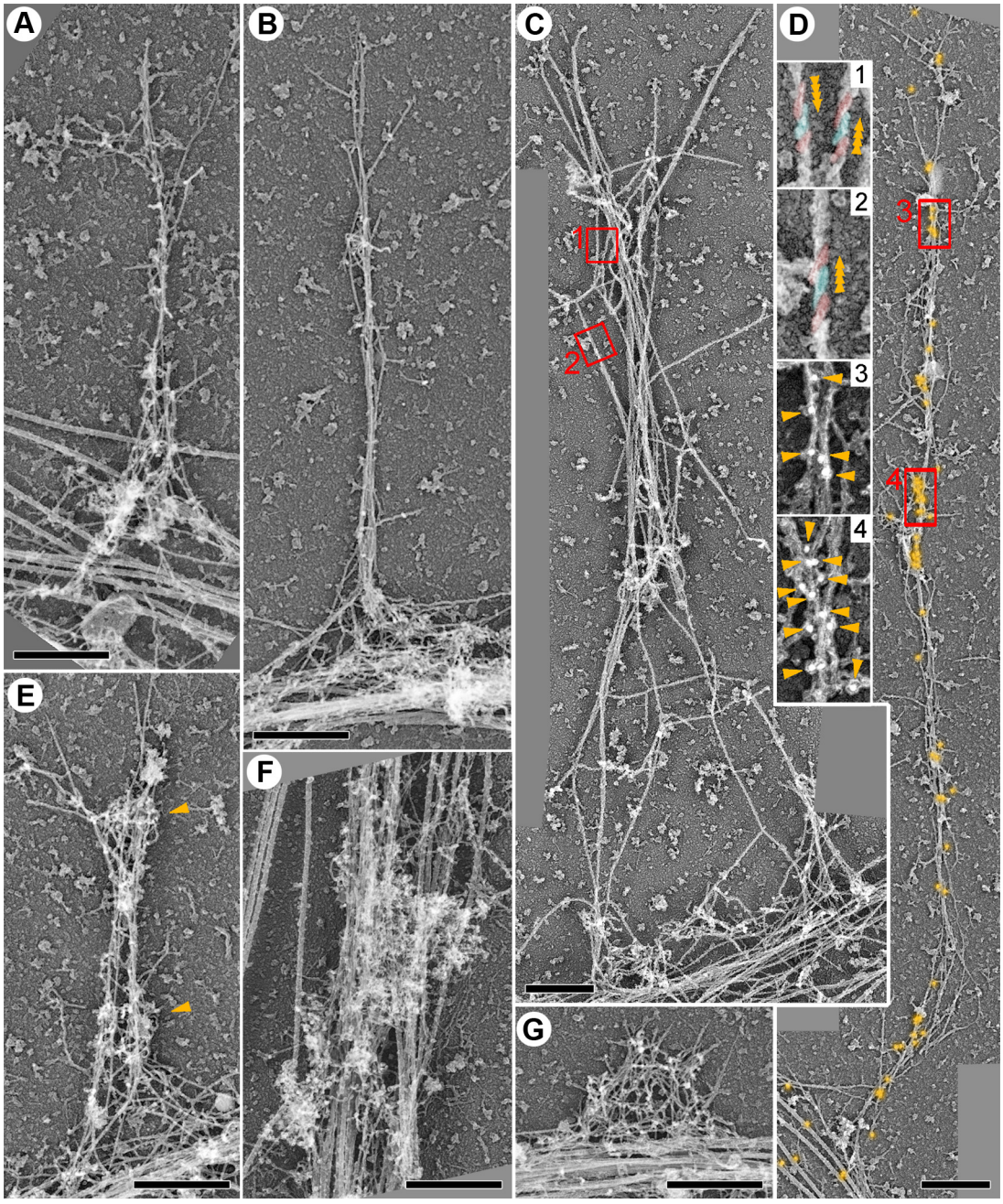

Figure 6. Cytoskeletal organization of dendritic filopodia and patches. EM of extracted 10 DIV hippocampal neurons. (A) A typical filopodium containing actin network in the base and the shaft. (B) A rare type of filopodia with a relatively well-shaped actin filament bundle, which however contains branched filaments and linear filaments of variable lengths. (C) S1 decorated filopodium. Red boxes 1 and 2 are enlarged in numbered panels at right to show actin filaments of mixed polarity. Adjacent asymmetric units of S1 decoration are highlighted in alternating red and cyan colors. The compound orange arrowheads point toward the pointed ends of filaments. (D) Filopodium stained with myosin II antibody contains gold particles (orange) distributed along the length as linear clusters (boxes) or single particles. Red boxes 3 and 4 are enlarged in panels with corresponding numbers at left to show noncolorized gold particles (arrowheads). (E) Filopodium containing prominent patches of branched actin network at the tip and in the lower shaft (arrowheads). (F and G) Dendritic patches of branched actin network with three-dimensional (F) or flattened (G) morphology. Bars, 0.5 μm.

osin II filaments, whereas in the head they were usually scattered as single particles (Figure 5D).

Actin Cytoskeleton Organization and Cytoskeletal Components in Dendritic Filopodia

The dendritic filopodia were investigated by replica EM by using 10 DIV hippocampal neurons (Figure 6). Their structure was strikingly different from that of conventional filopodia (Svitkina *et al.*, 2003; Korobova and Svitkina, 2008), but similar to that of spine necks. It consisted of loosely aligned actin filaments of varying length with some branched filaments and occasional bundles (Figure 6, A and B). In addition, patches of a branched network were associated with filopodial shafts and even more frequently with filopodial

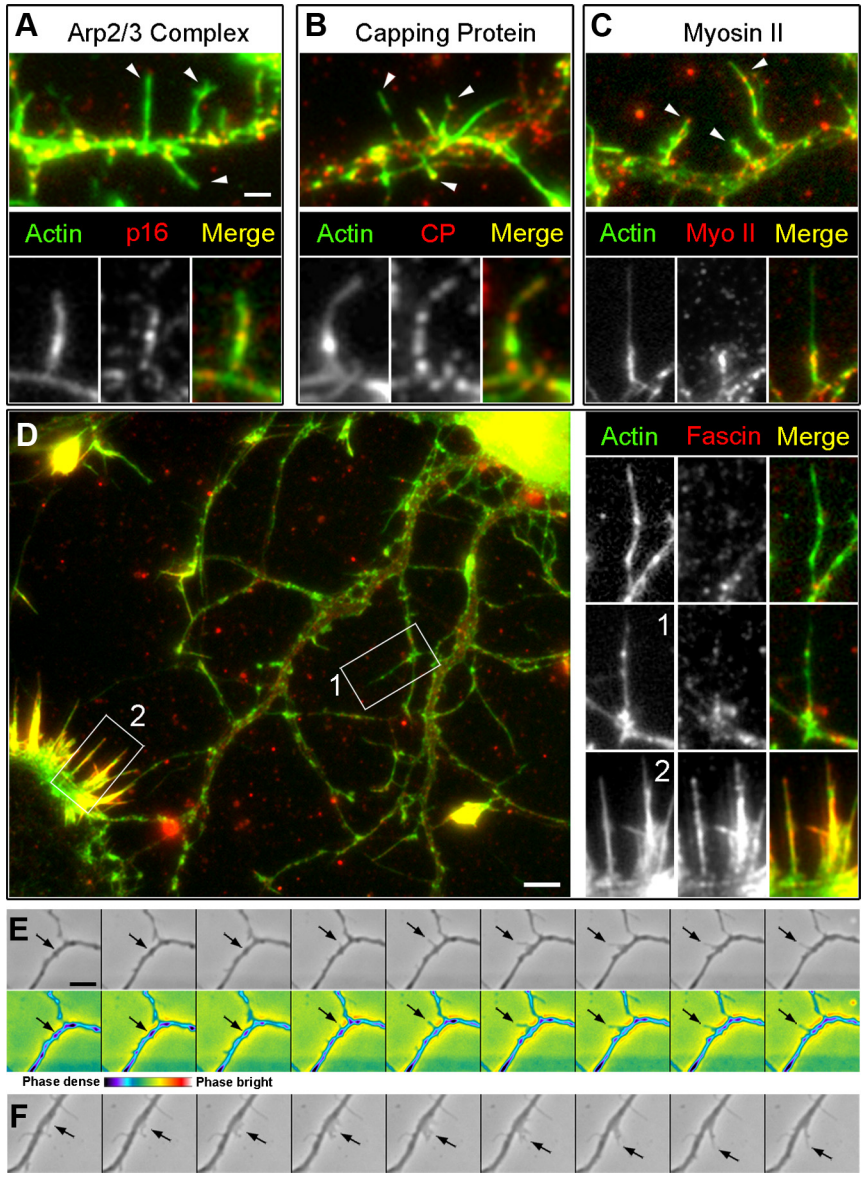

Figure 7. Molecular markers and dynamics of dendritic filopodia. (A–D) Fluorescence staining of cytoskeletal components in filopodia of 7–11 DIV hippocampal neurons by phalloidin (green) and indicated antibodies (red) shown at low magnification (top, A–C, left, D) or high magnification (bottom, A–C, right, D). Dendritic filopodia in A–C are indicated by arrowheads. Boxes 1 and 2 from D are enlarged in side panels with corresponding numbers. Unlabeled top panel shows a dendritic filopodium from another dendrite. Box 2 shows fascin-positive growth cone filopodia in contrast to dendritic filopodia not containing significant amounts of fascin. (E and F) Time-lapse phase-contrast sequences showing initiation of dendritic filopodia (arrows) from phase-dense spots (E) or small lamellipodia (F) in 10 DIV neurons. Bottom panel in E shows a color-coded image from the top panel to emphasize the phase-dense patches (purple). Time intervals are 6 s (E) or 3 s (F). Bars, 2 μm (A–C), 5 μm (F), and 5 μm (E and F).

tips producing prominent bulges there (Figure 6, A and E). The base of dendritic filopodia was similar to that of spines, both in the shape and cytoskeletal organization (Figure 6). Decoration of actin filaments with myosin S1 revealed a small fraction of actin filaments with barbed ends facing away from the tip (Figure 6C), which is unusual for conventional filopodia. Besides filopodia, patches of highly branched actin network, either relatively flat like in lamellipodia (Figure 6G), or more three-dimensional (Figure 6F), were associated with dendrites in these cultures.

By immunofluorescence staining, the Arp2/3 complex and capping protein were present in 65% (N = 54) and 69% (N = 74), respectively, of dendritic filopodia (Figure 7, A and B) unlike the conventional filopodia, which lack these proteins (Svitkina and Borisy, 1999; Svitkina *et al.*, 2003). Conversely, fascin was absent in dendritic filopodia, but abundant in conventional growth cone filopodia (Figure 7D). A majority of dendritic filopodia (88%; N = 77) contained myosin II, especially in the proximal regions (80% of the myosin II-positive filopodia) (Figure 7C). Immunogold EM with the myosin II antibody revealed both single gold particles and their linear clusters in dendritic filopodia (Figure 6D).

To understand how dendritic filopodia may be formed, we followed their dynamics in 10 DIV neuronal cultures by time-lapse phase-contrast microscopy. Filopodia usually originated from phase-dense dynamic patches or small lamellipodia associated with the dendritic shafts (Figure 7, E–F, and Supplemental Videos S1 and S2). These precursors of filopodia likely correspond to the patches of branched actin filaments we noted in EM samples (Figure 6F). Newly formed, as well as some preexisting filopodia, were highly dynamic, whereas other preexisting filopodia were stable and expressed relatively little dynamics. To address a possibility that stable and dynamic filopodia may differ in the contents of key cytoskeletal components, we evaluated the amounts of F-actin and the Arp2/3 complex by fluorescence microscopy in filopodia with pre-recorded behavior. Quantification of fluorescence intensities of filopodia stained with fluorescent phalloidin and Arp2/3 complex antibodies revealed no statistically significant differences in either F-actin or Arp2/3 contents between stable and dynamic filopodia

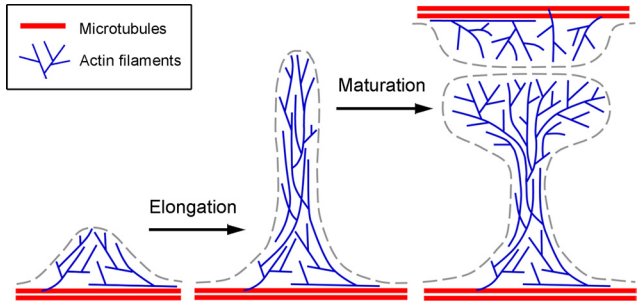

Figure 8. Model for actin cytoskeleton organization in dendritic protrusions and for spine morphogenesis. The actin cytoskeleton in dendritic patches (left), dendritic filopodia (middle), and dendritic spines (right) has similar organization consisting of a mixed network of linear and branched actin filaments (blue) anchored to microtubules (red) or actin filaments in the dendritic shaft. The process of spine formation probably begins with the formation of a dendritic patch, which then elongates into a dendritic filopodium. On receiving of appropriate signals, the filopodium undergoes maturation into a spine; this process probably involves activation of the Arp2/3 complex followed by formation of a dense branched actin network, which drives the expansion of the filopodial tip into a spine head. Presynaptic bouton forming a synapse with the spine head spine contains a similar network of actin filaments. Membrane is shown in gray.

(Supplemental Figure S7), consistent with our EM data showing comparable organization of the actin cytoskeleton in the entire population of filopodia.

DISCUSSION

Although the important role of dendritic spines in synaptic transmission is well established, the full understanding of their biology is critically delayed by the absence of their high-resolution structure. Diverse diagrams of the actin cytoskeleton organization in spines existing in the literature rather reflect a range of speculations than actual knowledge (Halpain, 2000; Rao and Craig, 2000; Ethell and Pasquale, 2005; Tada and Sheng, 2006), but they reveal how acutely this information is needed. In this study, we have characterized the cytoskeletal organization of dendritic spines and dendritic filopodia in their entirety and at high resolution and proposed a model of spine morphogenesis driven by actin cytoskeleton remodeling (Figure 8).

Dendritic Spines

Out of three structural domains of a mushroom spine, the base is a previously unrecognized compartment whose structure ranges from an elaborate mixture of branched and linear filaments to a few converging linear filaments. This variability resembles a situation with basal regions of conventional filopodia, in which fraction of linear filaments increases with filopodia maturation (Svitkina *et al*., 2003). This similarity suggests that the spine base may be a remainder of a precursor structure, which gradually changes its organization with its age.

The spine neck, unexpectedly, is supported not by an axial bundle of actin filaments, but by a longitudinally stretched network of branched and linear filaments of different lengths, which are only roughly aligned with each other. Although we cannot completely exclude a possibility that this structure is an artifact of the technique, there are several arguments against such possibility. First, by correlative EM we do not reveal significant reorganization and/or loss of actin in spines. Second, the presence of Arp2/3 complex and capping protein in spine necks is also consistent with their network-like organization. Third, replica technique successfully reveals long bundled filaments in other cases (Svitkina *et al*., 2003; Yang *et al*., 2007; Korobova and Svitkina, 2008). Finally, our results do not actually conflict with previous EM data obtained by other techniques showing occasional episodes of bundling by thin section EM (Fifkova and Delay, 1982; Markham and Fifkova, 1986) or roughly aligned filaments by freeze-fracture EM (Landis and Reese, 1983; Hirokawa, 1989). Because detection of branched filaments and filament ends in sectioned or fractured samples is difficult, replica EM of whole-mount samples used here provides more interpretable images.

The spine head undergoes constant actin-dependent shape changes (morphing), probably regulated by synaptic stimulation (Tada and Sheng, 2006; Bourne and Harris, 2008). Dynamic actin-dependent processes are frequently associated with branched actin networks nucleated by the Arp2/3 complex (Pollard and Borisy, 2003; Goley and Welch, 2006). Such networks were also expected to function in spine heads (see Introduction). Our data support these expectations by showing extensively branched actin network in the distal regions of spines.

Although replica EM is very beneficial for revealing the cytoskeletal architecture, it is limited by necessity to remove the plasma membrane to expose the cytoskeleton. Consequently, it is not possible to determine precisely where the spine head ends. To overcome this problem, at least partially, we used immunogold labeling of N-cadherin and PSD-95 in conditions that partly preserve these plasma membrane-associated components. These data allowed us to suggest that an apparently single piece of actin network connecting a spine to the axon, in fact, consists of pre- and postsynaptic subsets. This idea is more consistent with the available data, compared with an alternative possibility of actin filaments from the spine head directly interacting with axonal microtubules. Indeed, transmembrane adhesion receptors mediating cell–cell junctions usually interact through additional proteins with the actin cytoskeleton on both sides of the junction, rather than with microtubules. Furthermore, there is convincing evidence that presynaptic actin exists and is important for synaptic vesicle trafficking (Cingolani and Goda, 2008). Our data suggest that the presynaptic actin cytoskeleton consists of a branched actin network similar to that in the spine head and is also associated with microtubules.

In adaptive dynamic systems, like dendritic spines, protrusion and retraction cooperate in generating a proper shape, which may explain the presence of myosin II in spines (Morales and Fifkova, 1989; Ryu *et al*., 2006). We found that myosin II is biased toward the neck and proximal regions of the head, suggesting that contraction mainly occurs there. Filamentous myosin II in spines suggests the presence actin filaments of mixed polarity. However, we could not obtain enough filaments with interpretable polarity to test this prediction. Because the quality of decoration was good elsewhere, such as in growth cones, we assume that actin filaments in spines are overloaded with other actin-binding proteins preventing filament saturation with S1, as required for polarity determination.

Dendritic Filopodia and Spine Morphogenesis

Dendritic filopodia can transform into morphologically mature spines (Yoshihara *et al*., 2009). Their structure remained totally unknown but was assumed to resemble that of conventional filopodia. Strikingly, we found that dendritic

filopodia had network-like cytoskeletal organization, which is unusual for highly elongated membrane protrusions, where a tight actin filament bundle is considered to be obligatory (Chhabra and Higgs, 2007). However, we have shown recently that bundled actin filaments are dispensable for maintaining filopodia induced by the membrane-deforming I-BAR domain of IRSp53, although polymerized actin is required (Yang *et al*., 2009). Dendritic filopodia provide a naturally occurring example of this kind. The network-like organization of dendritic filopodia probably makes them more plastic allowing for frequent changes of direction (Portera-Cailliau *et al*., 2003).

The structural organization of dendritic filopodia suggests potential mechanisms of their differentiation into spines. By live imaging, the filopodium-to-spine transformation occurs as swelling of the filopodial tip and shortening (Marrs *et al*., 2001). The swelling may occur through Arp2/3 complex-dependent actin filament branching at the filopodial tip, which would drive the head expansion. Filopodia with sizable patches of branched actin network at the tip may represent transitional states in this process. The filopodia shortening during spine maturation was proposed to involve myosin II (Ryu *et al*., 2006). We indeed detected myosin II in the shafts of dendritic filopodia and also observed actin filaments of mixed polarity there. Both features are quite unusual for conventional filopodia, which are devoid of myosin II and have uniformly oriented filaments, but are consistent with contractile properties of dendritic filopodia.

Another important question is the origin of dendritic filopodia. By light microscopy, they seem to grow directly from a dendrite (Dailey and Smith, 1996), usually from pre-existing actin patches (Andersen *et al*., 2005) or, in our experiments, from phase-dense spots or small lamellipodia. These sites of filopodia initiation likely correspond to patches of a branched actin network in dendrites, which may subsequently become the filopodial base, thus explaining the presence of branched filaments there. These branched filaments may be responsible for incorporation of labeled actin into roots of dendritic filopodia (Hotulainen *et al*., 2009).

The mechanism of transformation of a relatively isometric patch into an elongated protrusion remains unclear. One possibility is contribution of membrane-deforming proteins, such as IRSp53 (Choi *et al*., 2005; Mattila and Lappalainen, 2008), which can induce and support tubular membrane protrusions (Saarikangas *et al*., 2009; Yang *et al*., 2009). Enhanced polymerization of actin filaments assisted by formin mDia2 may also contribute to this process (Hotulainen *et al*., 2009).

Surprisingly, the actin structures in neurons frequently reside directly on the microtubule array. Moreover, some actin filaments seem to branch off of a microtubule in the neurite suggesting involvement of a microtubule-associated actin filament nucleator(s) or actin–microtubule cross-linkers, which remain to be identified. In conclusion, the cytoskeletal organization and molecular composition of dendritic spines and dendritic filopodia suggest a likely sequence of cytoskeletal reorganizations underlying the spine morphogenesis (Figure 8). We propose that the process begins with the formation of a small patch of branched actin network, which might be nucleated in association with dendritic microtubules. The patch subsequently elongates into a dendritic filopodium, which due to plastic network-like organization of its cytoskeleton is able to perform a wide range of movements searching for an axon. When an appropriate signal is received, it triggers the head formation by inducing extensive branching of actin filaments. Myosin II-dependent contractility within the head and the neck then modulates the shape of the spine to fit the requirements of synaptic transmission. This model provides a conceptual framework for future studies which would uncover structural reorganizations of the cytoskeleton occurring at different stages of synapse morphogenesis and specific roles of individual proteins in these processes.

ACKNOWLEDGMENTS

We thank Drs. M. A. Dichter, D. A. Schafer, W. J. Nelson, and L. G. Tilney for generous gifts of reagents and cells and D. Zinshteyn for technical assistance. This work is supported by National Institutes of Health grants GM-70898 and RR-22482 (to T. S.).

REFERENCES

Ackermann, M., and Matus, A. (2003). Activity-induced targeting of profilin and stabilization of dendritic spine morphology. Nat. Neurosci. *6*, 1194–1200.

Andersen, R., Li, Y., Resseguie, M., and Brenman, J. E. (2005). Calcium/calmodulin-dependent protein kinase II alters structural plasticity and cytoskeletal dynamics in *Drosophila*. J. Neurosci. *25*, 8878–8888.

Arellano, J. I., Benavides-Piccione, R., Defelipe, J., and Yuste, R. (2007). Ultrastructure of dendritic spines: correlation between synaptic and spine morphologies. Front. Neurosci. *1*, 131–143.

Bourne, J. N., and Harris, K. M. (2008). Balancing structure and function at hippocampal dendritic spines. Annu. Rev. Neurosci. *31*, 47–67.

Caceres, A., Banker, G., Steward, O., Binder, L., and Payne, M. (1984). MAP2 is localized to the dendrites of hippocampal neurons which develop in culture. Brain Res. *315*, 314–318.

Calabrese, B., Wilson, M. S., and Halpain, S. (2006). Development and regulation of dendritic spine synapses. Physiology *21*, 38–47.

Cheng, X. T., Hayashi, K., and Shirao, T. (2000). Non-muscle myosin IIB-like immunoreactivity is present at the drebrin-binding cytoskeleton in neurons. Neurosci. Res. *36*, 167–173.

Chhabra, E. S., and Higgs, H. N. (2007). The many faces of actin: matching assembly factors with cellular structures. Nat. Cell Biol. *9*, 1110–1121.

Choi, J., Ko, J., Racz, B., Burette, A., Lee, J. R., Kim, S., Na, M., Lee, H. W., Kim, K., Weinberg, R. J., and Kim, E. (2005). Regulation of dendritic spine morphogenesis by insulin receptor substrate 53, a downstream effector of Rac1 and Cdc42 small GTPases. J. Neurosci. *25*, 869–879.

Cingolani, L. A., and Goda, Y. (2008). Actin in action: the interplay between the actin cytoskeleton and synaptic efficacy. Nat. Rev. Neurosci. *9*, 344–356.

Dailey, M. E., and Smith, S. J. (1996). The dynamics of dendritic structure in developing hippocampal slices. J. Neurosci. *16*, 2983–2994.

Ethell, I. M., and Pasquale, E. B. (2005). Molecular mechanisms of dendritic spine development and remodeling. Prog. Neurobiol. *75*, 161–205.

Fifkova, E., and Delay, R. J. (1982). Cytoplasmic actin in neuronal processes as a possible mediator of synaptic plasticity. J. Cell Biol. *95*, 345–350.

Goley, E. D., and Welch, M. D. (2006). The ARP2/3 complex: an actin nucleator comes of age. Nat. Rev. Mol. Cell Biol. *7*, 713–726.

Halpain, S. (2000). Actin and the agile spine: how and why do dendritic spines dance? Trends Neurosci. *23*, 141–146.

Hering, H., and Sheng, M. (2003). Activity-dependent redistribution and essential role of cortactin in dendritic spine morphogenesis. J. Neurosci. *23*, 11759–11769.

Hirokawa, N. (1989). The arrangement of actin filaments in the postsynaptic cytoplasm of the cerebellar cortex revealed by quick-freeze deep-etch electron microscopy. Neurosci. Res. *6*, 269–275.

Honkura, N., Matsuzaki, M., Noguchi, J., Ellis-Davies, G. C., and Kasai, H. (2008). The subspine organization of actin fibers regulates the structure and plasticity of dendritic spines. Neuron *57*, 719–729.

Hotulainen, P., Llano, O., Smirnov, S., Tanhuanpaa, K., Faix, J., Rivera, C., and Lappalainen, P. (2009). Defining mechanisms of actin polymerization and depolymerization during dendritic spine morphogenesis. J. Cell Biol. *185*, 323–339.

Kim, Y., *et al*. (2006). Phosphorylation of WAVE1 regulates actin polymerization and dendritic spine morphology. Nature *442*, 814–817.

Korobova, F., and Svitkina, T. (2008). Arp2/3 complex is important for filopodia formation, growth cone motility, and neuritogenesis in neuronal cells. Mol. Biol. Cell *19*, 1561–1574.

Landis, D. M., and Reese, T. S. (1983). Cytoplasmic organization in cerebellar dendritic spines. J. Cell Biol. *97*, 1169–1178.

Markham, J. A., and Fifkova, E. (1986). Actin filament organization within dendrites and dendritic spines during development. Brain Res. *392*, 263–269.

Marrs, G. S., Green, S. H., and Dailey, M. E. (2001). Rapid formation and remodeling of postsynaptic densities in developing dendrites. Nat. Neurosci. *4*, 1006–1013.

Mattila, P. K., and Lappalainen, P. (2008). Filopodia: molecular architecture and cellular functions. Nat. Rev. Mol. Cell Biol. *9*, 446–454.

Matus, A. (2005). Growth of dendritic spines: a continuing story. Curr. Opin. Neurobiol. *15*, 67–72.

Morales, M., and Fifkova, E. (1989). In situ localization of myosin and actin in dendritic spines with the immunogold technique. J. Comp. Neurol. *279*, 666–674.

Papa, M., Bundman, M. C., Greenberger, V., and Segal, M. (1995). Morphological analysis of dendritic spine development in primary cultures of hippocampal neurons. J. Neurosci. *15*, 1–11.

Pollard, T. D., and Borisy, G. G. (2003). Cellular motility driven by assembly and disassembly of actin filaments. Cell *112*, 453–465.

Portera-Cailliau, C., Pan, D. T., and Yuste, R. (2003). Activity-regulated dynamic behavior of early dendritic protrusions: evidence for different types of dendritic filopodia. J. Neurosci. *23*, 7129–7142.

Racz, B., and Weinberg, R. J. (2006). Spatial organization of cofilin in dendritic spines. Neuroscience *138*, 447–456.

Racz, B., and Weinberg, R. J. (2008). Organization of the Arp2/3 complex in hippocampal spines. J. Neurosci. *28*, 5654–5659.

Rao, A., and Craig, A. M. (2000). Signaling between the actin cytoskeleton and the postsynaptic density of dendritic spines. Hippocampus *10*, 527–541.

Ryu, J., Liu, L., Wong, T. P., Wu, D. C., Burette, A., Weinberg, R., Wang, Y. T., and Sheng, M. (2006). A critical role for myosin IIb in dendritic spine morphology and synaptic function. Neuron *49*, 175–182.

Saarikangas, J., Zhao, H., Pykalainen, A., Laurinmaki, P., Mattila, P. K., Kinnunen, P. K., Butcher, S. J., and Lappalainen, P. (2009). Molecular mechanisms of membrane deformation by I-BAR domain proteins. Curr. Biol. *19*, 95–107.

Sheng, M., and Hoogenraad, C. C. (2007). The postsynaptic architecture of excitatory synapses: a more quantitative view. Annu. Rev. Biochem. *76*, 823–847.

Small, J. V., Stradal, T., Vignal, E., and Rottner, K. (2002). The lamellipodium: where motility begins. Trends Cell Biol. *12*, 112–120.

Svitkina, T. (2007). Electron microscopic analysis of the leading edge in migrating cells. Methods Cell Biol. *79*, 295–319.

Svitkina, T. M., and Borisy, G. G. (1999). Arp2/3 complex and actin depolymerizing factor/cofilin in dendritic organization and treadmilling of actin filament array in lamellipodia. J. Cell Biol. *145*, 1009–1026.

Svitkina, T. M., Bulanova, E. A., Chaga, O. Y., Vignjevic, D. M., Kojima, S., Vasiliev, J. M., and Borisy, G. G. (2003). Mechanism of filopodia initiation by reorganization of a dendritic network. J. Cell Biol. *160*, 409–421.

Svitkina, T. M., Verkhovsky, A. B., McQuade, K. M., and Borisy, G. G. (1997). Analysis of the actin-myosin II system in fish epidermal keratocytes: mechanism of cell body translocation. J. Cell Biol. *139*, 397–415.

Tada, T., and Sheng, M. (2006). Molecular mechanisms of dendritic spine morphogenesis. Curr. Opin. Neurobiol. *16*, 95–101.

Verkhovsky, A. B., Surgucheva, I. G., Svitkina, T. M., Tint, I. S., and Gelfand, V. I. (1987). Organization of stress fibers in cultured fibroblasts after extraction of actin with bovine brain gelsolin-like protein. Exp. Cell Res. *173*, 244–255.

Verkhovsky, A. B., Svitkina, T. M., and Borisy, G. G. (1995). Myosin II filament assemblies in the active lamella of fibroblasts: their morphogenesis and role in the formation of actin filament bundles. J. Cell Biol. *131*, 989–1002.

Vignjevic, D., Yarar, D., Welch, M. D., Peloquin, J., Svitkina, T., and Borisy, G. G. (2003). Formation of filopodia-like bundles in vitro from a dendritic network. J. Cell Biol. *160*, 951–962.

Wegner, A. M., Nebhan, C. A., Hu, L., Majumdar, D., Meier, K. M., Weaver, A. M., and Webb, D. J. (2008). N-WASP and the Arp2/3 complex are critical regulators of actin in the development of dendritic spines and synapses. J. Biol. Chem. *283*, 15912–15920.

Wilcox, K. S., Buchhalter, J., and Dichter, M. A. (1994). Properties of inhibitory and excitatory synapses between hippocampal neurons in very low density cultures. Synapse *18*, 128–151.

Wyszynski, M., Lin, J., Rao, A., Nigh, E., Beggs, A. H., Craig, A. M., and Sheng, M. (1997). Competitive binding of alpha-actinin and calmodulin to the NMDA receptor. Nature *385*, 439–442.

Yang, C., Czech, L., Gerboth, S., Kojima, S., Scita, G., and Svitkina, T. (2007). Novel roles of formin mDia2 in lamellipodia and filopodia formation in motile cells. PLoS Biol. *5*, e317.

Yang, C., Hoelzle, M., Disanza, A., Scita, G., and Svitkina, T. (2009). Coordination of membrane and actin cytoskeleton dynamics during filopodia protrusion. PLoS One *4*, e5678.

Yoshihara, Y., De Roo, M., and Muller, D. (2009). Dendritic spine formation and stabilization. Curr. Opin. Neurobiol. *19*, 146–153.